PRAMANA
— journal of
physics

Vol. 67, No. 2
August 2006
pp. 257–268

Elliptic flow in a hadron-string cascade model at 130 GeV energy

P K SAHU[1], A OHNISHI[2], M ISSE[2], N OTUKA[3] and S C PHATAK[1]
[1]Institute of Physics, Sachivalaya Marg, Bhubaneswar 751 005, India
[2]Division of Physics, Graduate School of Science, Hokkaido University, Sapporo 060-0810, Japan
[3]Nuclear Data Center, Department of Nuclear Energy System, Japan Atomic Energy Research Institute, Tokai, Ibaraki 319-1195, Japan

MS received 1 July 2005; revised 19 January 2006; accepted 15 March 2006

Abstract. We present the analysis of elliptic flow at $\sqrt{s}$ = 130 A GeV energy in a hadron-string cascade model. We find that the final hadronic yields are qualitatively described. The elliptic flow v_2 is reasonably well-described at low transverse momentum ($p_T < 1$ GeV/c) in mid-central collisions. On the other hand, this model does not explain v_2 at high p_T or in peripheral collisions and thus generally, it underestimates the elliptic flow at RHIC energy.

Keywords. Heavy-ion collisions; elliptic flow.

PACS Nos 25.75.-q; 24.10.-i; 24.85.+p

1. Introduction

In high-energy heavy-ion collisions, strongly interacting matter at high temperature and/or density is created. When two nuclei collide, nucleon–nucleon (NN) interactions produce large number of particles – hadrons, strings and partons – and these particles will develop collectivity and eventually thermalize. The prime aim of high-energy heavy-ion collisions is to explore the properties of this extreme state of matter far from stable nuclei. Especially the confirmation of the deconfined phase of quarks and gluons, e.g., quark-gluon plasma (QGP) [1] is of current interest. Although it is not straightforward to connect the observable in heavy-ion collision experiments with the properties of matter under equilibrium, several observables such as collective flows have been proposed to be sensitive to these properties [2,3].

Recent RHIC experiments [4–13] have shown that radial and elliptic flows are strongly generated. Both these flows are studied using hydrodynamic model [14–19] for different hadron species produced in Au + Au collisions at $\sqrt{s}$ = 19.6–200 A GeV. Among these, the elliptic flow (v_2) has attracted much attention at high incident energies, and it is measured in a wide energy range from GSI-SIS

(∼1 A GeV) [20], BNL-AGS (2–10.6 A GeV) [21], to CERN-SPS (40–158 A GeV) [22], in addition to BNL-RHIC. In non-central collisions, collective flow is characterized by the azimuthal correlations between particle momenta and the reaction plane, which is defined by the incident momentum and the impact parameter vectors **b**. The elliptic flow v_2 is the anisotropy of particle emission in- and out-of reaction plane. In non-central collisions of heavy nuclei, the nucleus–nucleus overlap initially is lens- or almond-shaped. This spatial anisotropy creates stronger pressure gradient in in-plane direction than in out of plane direction by re-scatterings, provided the squeezing from spectators are negligible. Since the almond shape is obscured in the later stage, strong v_2 is generally believed to be an evidence of early thermalization. For example, to explain the strong elliptic flow at RHIC, it is required to set the thermalization time of the order of 1 fm/c in hydrodynamical [14] studies.

The above considerations imply the importance of partonic interactions in the early stage at RHIC. Hadrons are mainly produced through the fragmentation of jets or strings after the formation time $\tau_{\rm f} \sim 1$ fm/c. Strings are often considered to interact before hadronization only when they contain constituent quarks of the original hadron [23,24]. Thus most of the hadrons, made of created $\bar{q}q$, have to wait for $\tau_{\rm f}$ before re-scattering. On the other hand, partons can make re-scatterings in the early stages within the hadron formation time. Since the number of freed partons in the primary nucleon–nucleon interaction is expected to be much larger at RHIC than at SPS, we expect significant difference in the elliptic flow as a function of the transverse momentum, because some of the particles are present at high transverse momenta at RHIC energy due to hard gluon–gluon scattering, and the high $p_{\rm T}$ particles go off the reaction zone quickly, and thus their elliptic flow reflects early stage thermalization. However, recent observation at SPS shows similar behaviour of the elliptic flow like RHIC as a function of the particle transverse momentum [22]. In addition, there are some reports in which the elliptic flow at RHIC is underestimated in hadron-string cascade models [25–27]. In order to reproduce the flow, the strings had to be melted to partons again and the partons had to scatter with a cross-section of 6–8 mb [27]. Therefore, there is a possibility that the strong elliptic flow at RHIC may or may not be a consequence of partonic interactions in the early stage. In order to clarify this point, it is necessary to understand the mechanism of strong elliptic flow generated at RHIC, and examine the elliptic flow at SPS energies in comparison with that at RHIC in hadron-string cascade models.

Another interesting point is the method of extracting v_2. In a standard method in experimental data analyses [28], the reaction plane is determined from particle momentum distribution, and v_2 is calculated using the azimuthal angle with respect to this reaction plane. In the standard treatment, there are several sources of non-flow contributions such as the resonance decays, jets, mini-jets and Coulomb interaction. Also, v_2 values are extracted from particle azimuthal angle correlations and they are compared with the reaction plane method [29]. While the results from the reaction plane and particle correlation methods seem to be in agreement within the error bars, the four-particle correlations significantly reduce the non-flow contribution compared to the two-particle correlations. In the reaction plane method, particles from mini-jets are also used to estimate the reaction plane, and thus the reaction plane is correlated with mini-jets. Thus it is also interesting to

compare v_2 values using the two methods in the model calculations for SPS and RHIC energies.

In this paper, we analyze the elliptic flow in heavy-ion collisions at RHIC energy of $\sqrt{s_{NN}} = 130$ GeV in a hadron-string cascade model with jet production (JAM) [24,30]. We will show that final hadronic yield ($\mathrm{d}N/\mathrm{d}\eta$ and p_T distribution) at RHIC are roughly explained in JAM. In addition, the elliptic flow (v_2) at low p_T ($p_\mathrm{T} < 1$ GeV/c) in mid-central collisions (centrality $< 20\%$) is reasonably well-described. However, v_2 value is decreased at high transverse momentum or in peripheral collisions. As a result, this model undervalues v_2 as a function of pseudo-rapidity by about 30% and v_2 as a function of transverse momentum for $p_\mathrm{T} > 0.5$ GeV/c, for minimum bias events. Next we compare the elliptic flows at SPS and RHIC energies. Calculated results as well as the experimental data show that the transverse momentum dependence of the elliptic flow at SPS is very similar to that at RHIC. The similarity in the present hadron-string cascade model comes from the late growth of the elliptic flow, $t \sim 10$ fm/c. Since the transverse momentum is generally much smaller than the longitudinal momentum in string fragmentation, the spatial ellipticity does not become very small when hadrons are formed. If this late growth is the true mechanism to enhance the elliptic flow, it becomes almost a flat function of the (pseudo)rapidity. The data from the PHOBOS Collaboration [12] do not necessarily support this behaviour. We also compare the v_2 values calculated in the reaction plane method and two-particle correlation method. It is found that the two methods give similar values in JAM, while they give significantly different results in a model without hadronic re-scatterings.

2. Transport model and elliptic flow calculation

In order to analyze high-energy heavy-ion collisions, many cascade-type models have been developed up to SPS energies and have met with some successes in explaining the data [31,30]. The most basic feature of hadronic cascade models is the implementation of hadron–hadron elementary cross-sections. At low energies, pions are mainly produced through resonance formation and decay. At medium energies ($\sqrt{s} = 3$–10 GeV), string formation and decay becomes dominant [23,24,32–34]. There are some models in which multi-pions are directly produced according to the parametrization of experimental data [35], or by using multi-particle production model such as the multi-chain model [36]. At high energies ($\sqrt{s} \geq 20$ GeV), partonic interactions becomes important especially in describing high p_T hadrons. Jet production is estimated by folding the partonic pQCD cross-sections with parton distribution in hadrons [32,37]. In describing the elliptic flow at RHIC, we believe that all the above processes have to be included. In the nucleon–nucleon (NN) collisions at $\sqrt{s_{NN}} = 130$ GeV, jet production (hard process) cross-section amounts to around 15% of the total cross-section, and the rest of the NN cross-section is dominated by the string formation, then both of these processes are required at the first chance NN collisions during the nucleus–nucleus (AA) collisions. Low-energy hadron–hadron collisions are also necessary, since they are responsible for the later thermalizations in AA collisions.

The next important feature in cascade models is the way to treat multiple scatterings. In principle, each particle–particle collision is regarded as an incoherent process in cascade models, but several coherent effects have been found to be important. One of them is the re-scattering of strings containing constituent quarks in the original hadron. This effect is pointed out by Sorge [23] in the analysis of proton rapidity distribution at SPS; if a string produced in the primary NN collision does not interact before hadronization, the di-quark in the baryonic string would have almost the same velocity as the incident nucleon, then the stopping power at SPS cannot be explained.

In this work, we analyze the elliptic flow using a hadron-string cascade simulation model, JAM [24]. The main features of this model are as follows: (1) At low energies ($\sqrt{s} < 4$–5 GeV), inelastic hadron–hadron collisions are modeled by the resonance productions based on the idea from RQMD [23,33] and UrQMD [34]. (2) Above the resonance region, soft string excitation is implemented along the lines of the HIJING model [37]. String fragmentation to hadrons is calculated in the Lund fragmentation model, using PYTHIA program [32]. (3) String interaction before hadronization is simulated by the re-scattering of hadrons having original constituent quarks within a formation time, assuming the additive quark model cross-section. (4) Multiple mini-jet production is included in the same way as the HIJING model. Jet production cross-section and the number of jets are calculated using an eikonal formalism for perturbative QCD (pQCD) and hard parton–parton scatterings with initial and final state radiation simulated using PYTHIA [32] program. Produced mini-jets later fragment to hadrons through string configurations. (5) Mini-jet production in NN collision is regarded as independent, and the coherence between different nucleons is not taken into account. (6) Parton re-scattering among different mini-jets are not included. The detailed description of this model is given in refs [24,30]

The first three points are the most dominating part in the present calculation at RHIC. However, the effect to the present calculation by the latter three points is insignificant. These are evident in the results and are discussed in the next section.

The elliptic flow v_2 is defined as the second Fourier component in the azimuthal angle distribution relative to the reaction plane as defined by

$$\frac{\mathrm{d}N(\eta, p_\mathrm{T})}{\mathrm{d}\phi} = v_0(1 + 2v_1\,\cos\phi + 2v_2\cos 2\phi + \cdots)\ . \tag{1}$$

If we know the true reaction plane, we can easily calculate v_2 using the final state hadron momenta as

$$v_2(\eta, p_\mathrm{T}) = \langle\cos 2\phi\rangle = \left\langle\frac{p_x^2 - p_y^2}{p_x^2 + p_y^2}\right\rangle . \tag{2}$$

While in a model calculation we know the true reaction plane, it is not obvious in experiments. One of the way to estimate v_2 without the knowledge of the true reaction plane is to use the two-particle correlation [38]

$$\begin{aligned}\langle\cos 2\,(\phi_i - \phi_j)\rangle &= \langle\cos 2\phi_i\rangle\langle\cos 2\phi_j\rangle + \langle\sin 2\phi_i\rangle\langle\sin 2\phi_j\rangle \\ &= v_2(\eta_1, p_{\mathrm{T}1})\, v_2(\eta_2, p_{\mathrm{T}2})\ ,\end{aligned} \tag{3}$$

where the average is taken over particles with the condition $(\eta_i, p_{\mathrm{T}i}) = (\eta_1, p_{\mathrm{T}1})$ and $(\eta_j, p_{\mathrm{T}j}) = (\eta_2, p_{\mathrm{T}2})$.

3. Results

We have generated around 10k minimum bias ($0 < b < 13$ fm) simulation events at RHIC energy ($\sqrt{s} = 130$ A GeV), and 5k events at SPS energy ($\sqrt{s} = 17$ A GeV ($E_{\mathrm{inc}} = 158$ A GeV)). Default parameters in JAM are adopted except for a little wider p_{T} width in the string decay and a larger partonic minimum p_{T} ($p_0 = 2.7$ GeV/c) to get a stiffer p_{T} distribution of charged particles in pp collisions at RHIC. Phase-space coordinates of the final collision/decay points are recorded, and v_2 values are calculated later using the phase-space data. In central or mid-central collisions, we choose impact parameter range corresponding to experimental centrality (i.e., centrality $= \pi b^2/\sigma_{\mathrm{geo}}$, where $\sigma_{\mathrm{geo}} = 720$ fm^2) in Au+Au collisions [9].

First we show the pseudo-rapidity η distribution of charged particles at RHIC energy ($\sqrt{s_{NN}} = 130$ GeV) in the upper panel of figure 1. Calculated charged hadron distribution explains well the PHOBOS data at large η for central collisions [11], although we find a slight overestimation at mid-rapidities compared to the PHOBOS [11], BRAHMS [13], and PHENIX [9] data. This trend applies to mid-central collisions as well.

In the lower panel of figure 1, we show the calculated elliptic flow of charged particles for 5–53% and minimum bias events as a function of η in comparison with

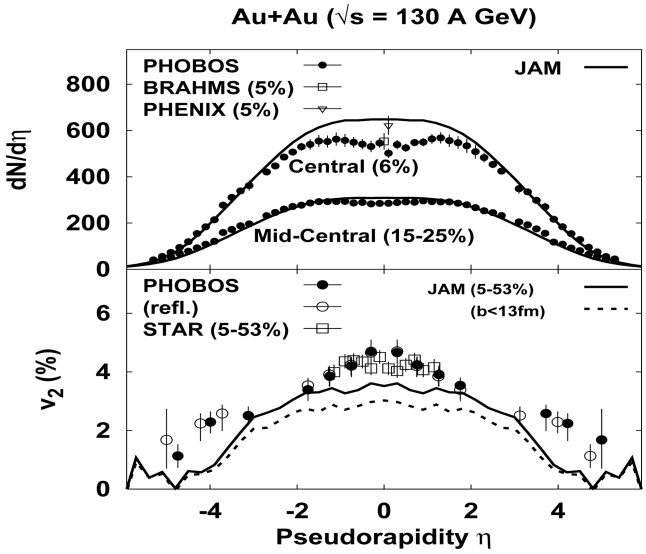

Figure 1. Pseudo-rapidity dependence of charged particle $\mathrm{d}N/\mathrm{d}\eta$ (upper panel for minimum bias events) and v_2 (lower panel for minimum bias events as well as 5–53% centrality) at RHIC ($\sqrt{s_{NN}} = 130$ GeV) in comparison with PHOBOS [11,12], BRAHMS [13], (5% centrality), PHENIX [9] (5% centrality), and STAR [4,5] (5–53% centrality) data.

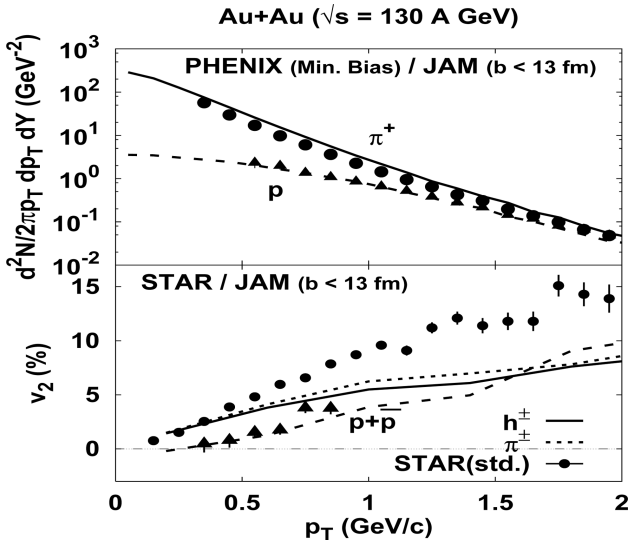

Figure 2. Transverse momentum p_{T} distribution (upper panel) and p_{T} dependence of v_2 (lower panel) for minimum bias events at RHIC ($\sqrt{s_{NN}} = 130$ GeV) in comparison with PHENIX [10] and STAR [5] data.

data from PHOBOS [12] and STAR [4,5,8] Collaborations at RHIC energy ($\sqrt{s_{NN}} =$ 130 GeV). The data from STAR [8] are not from the minimum bias but from 5–53% of the total hadronic cross-section and from the four-particle correlations. At mid-rapidity, the calculated v_2 undervalues the data by about 30%. In addition, the present model shows flat v_2 behaviour at $|\eta| < 2$, which contradicts the enhancement at small η observed by PHOBOS Collaboration [12].

In the upper panel of figure 2, we show the calculated p_{T} spectra of pions and protons at mid-rapidities for minimum bias events in comparison with data from PHENIX Collaboration at RHIC energy ($\sqrt{s_{NN}} = 130$ GeV) [10]. Pion and proton p_{T} spectra are reproduced qualitatively.

In the lower panel of figure 2, we display JAM results on elliptic flow of charged particles as functions of transverse momenta for minimum bias events at RHIC energy. In this figure, we notice that our model gives a reasonable description of the data in the low p_{T} region ($p_{\mathrm{T}} < 0.5$ GeV/c). For $p_{\mathrm{T}} > 0.5$ GeV/c, however, our v_2 values decrease by about 10–40% for charged particles.

Another interesting point to be noticed here is that the calculated elliptic flow is sensitive to the particle masses as a function of p_{T}. The particles which are having smaller masses such as pions and kaons have higher values of elliptic flow at small p_{T}, and these are linear functions of p_{T}. For higher mass particles such as protons, v_2 behaves non-linearly with p_{T}. Similar characteristics are observed in the STAR data [5] as well.

Figure 3 shows the centrality dependence of the elliptic flow. The data are taken from STAR Collaboration, where re-analyzed data by using cumulant methods for 4 particles show smaller values of v_2 than in the reaction plane method [8]. Our model (solid line) explains the data in mid-central region (centrality < 20%), but it

Elliptic flow at $\sqrt{s} = 130$ *A GeV*

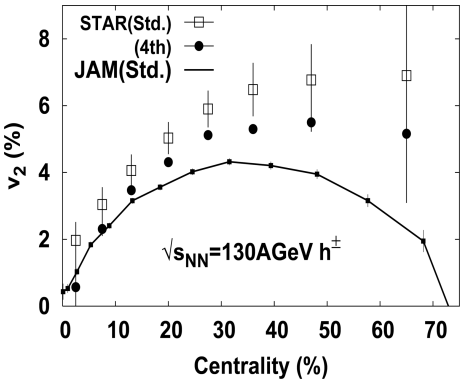

Figure 3. Calculated centrality dependence of v_2 at RHIC ($\sqrt{s_{NN}} = 130$ GeV) in comparison with STAR [8] data.

undervalues the data in peripheral collisions. This underestimation may be due to the lack of re-scattering of partons and interaction between hadrons and partons.

We compare our results with hydrodynamical model. The results of hydrodynamic model has not been shown in the figures, but, we have discussed its qualitative results and compared with the hadron-string cascade model. Our results in the lower panel of figure 1 show flat elliptic flow at $|\eta| < 2$. This is not specific to our model. A full 3D hydrodynamical model, which explains the strong elliptic flow at mid-rapidities, also gives very flat elliptic flows and consequently overestimates the data at larger rapidities for all reasonable initial conditions [19] because of incomplete thermalization. For elliptic flow as a function of p_{T}, our model describes the data up to $p_{\mathrm{T}} < 0.5$ GeV/c for all charged particles in the minimum bias events as shown in the lower panel of figure 2. In case of the hydrodynamic model, the elliptic flow agrees well with data up to $p_{\mathrm{T}} \sim 1.5$ GeV in central and semi-central collisions [15], where the measured elliptic flow begins to show signs of saturation to some value whereas the hydrodynamic results keeps increasing. Thus the result of hydrodynamic model fails at high p_{T}, due to saturation and onset of hard processes and fails at peripheral collisions due to incomplete early-time thermalization. Depending on the different equation of state in the hydrodynamic calculation, the pion elliptic flow as a function of p_{T} shows excellent agreement with the data and independent of the equation of state. But the proton elliptic flow in the hydrodynamic model seems to favour the data and hence show the existence of a phase transition to quark gluon plasma. However, unlike the elliptic flow of charged particles and pions, the proton elliptic flow is sensitive to freeze-out temperature and details of initial distribution [14,16]. Also, the data show a strong mass dependence of elliptic flow as a function of p_{T}, for example, at small values of p_{T}, the particle with heavy mass shows smaller elliptic flow. This is typical to hydrodynamical models. Very recently, it has been shown [17] that with the initial velocity kick for the hydrodynamic model the elliptic flow for antiproton can be fitted reasonably well as a function of p_{T} but for pions, the model results are still far from the data at p_{T} about 1.0 GeV/c. Therefore, it is hard to draw any conclusion regarding hydrodynamical models. As a function of centrality, we can

describe the elliptic flow in our model up to 20% centrality as shown in figure 3. Similarly, the elliptic flow can be described as the data in central and semi-central collisions in the hydrodynamic model. But the prediction in the most peripheral region [14,16] in hydrodynamic model overpredicts the elliptic flow data due to the loss of a sufficient degree of thermalization. Hence, a large degree of thermalization is favoured in central collisions and the non-equilibrium effects are required to reduce v_2 in peripheral collisions.

Dependence of v_2 on the analysis method can appear in theoretical model results, too. While the reaction plane is given *a priori* by the incident momentum and the impact parameter directions, correlation coming from jets may modify the two-particle azimuthal angle correlation [38]. In figure 4, we show v_2 results at RHIC (Au+Au, $\sqrt{s_{NN}} = 130$ GeV) and SPS (Pb+Pb, $\sqrt{s_{NN}} = 17$ GeV) for mid-central collisions calculated using the standard reaction plane method ($v_2 = \langle \cos 2\phi \rangle$, solid line for RHIC, and dotted line for SPS) and the two-particle correlation method ($v_2^2 = \langle \cos 2(\phi_i - \phi_j) \rangle$, dashed line for RHIC). Two results at RHIC are in agreement with each other within the statistical error bar, and we find that the elliptic flows are similar at SPS and RHIC energies when we see them as a function of p_{T}. If the hadronic final state interaction is the main source of v_2, we expect a similar trend also at lower SPS energies. The results of standard reaction plane method are at about 10–20% below the experimental values for $p_{\mathrm{T}} > 1$ to 2 GeV/c, but results for the particle correlation method are in agreement with data within error bars.

We show pseudo-rapidity (η) dependence of charged hadron elliptic flow v_2 in mid-central ($4 < b < 8$ fm) collisions at RHIC (Au+Au, $\sqrt{s_{NN}} = 130$ GeV, solid line) and SPS (Pb+Pb, $\sqrt{s_{NN}} = 17$ GeV, dashed line) [30] in figure 5. It is noteworthy that the present model explains the elliptic flow data at SPS energies [30]. We find that elliptic flows at mid-rapidity have similar values for RHIC and SPS.

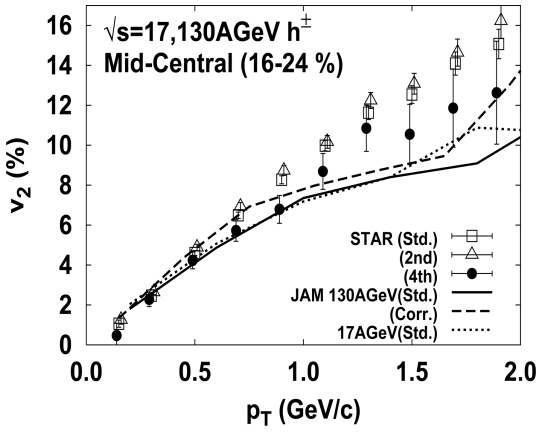

Figure 4. Elliptic flow calculated using the standard (reaction plane) method (solid line for RHIC, and dotted line for SPS) two-particle azimuthal angle correlation method (dashed line for the RHIC) in comparison with RHIC-STAR data in several analysis methods [8].

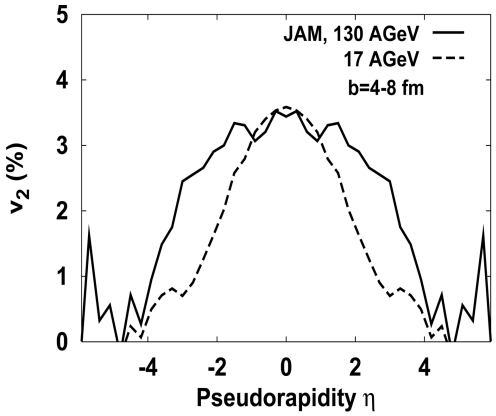

Figure 5. Calculated pseudo-rapidity (η) dependence of charged particle v_2 for mid-central (b = 4–8 fm) events at RHIC ($\sqrt{s_{NN}}$ = 130 GeV; solid line) and SPS ($\sqrt{s_{NN}}$ = 17 GeV; dashed line) energies.

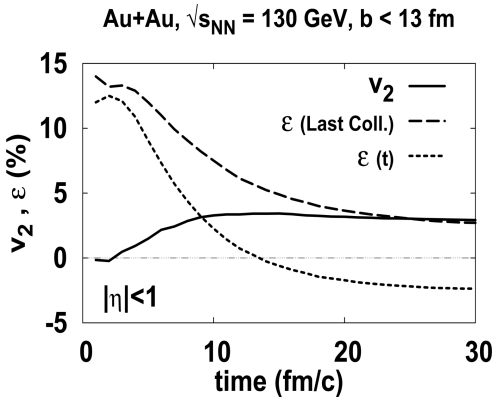

Figure 6. Time dependence of v_2 and ε for formed hadrons.

From the above analysis, one question arises: Why can the elliptic flow take similar values at RHIC and SPS energies in a hadronic cascade model? To answer this, we have made a simple time-dependent analysis. Elliptic flow is calculated as a function of time t for formed hadrons (after their formation time) in the pseudo-rapidity range $|\eta| < 1$, and is shown by the solid line in figure 6. It is found that v_2 grows slowly in the time $t < t_{v2} \simeq 10$ fm/c. For v_2 to grow, the spatial eccentricity, $\varepsilon = \langle (y^2 - x^2)/(y^2 + x^2) \rangle$, has to be finite. We show in figure 6 the eccentricity ε of formed hadrons at time t ($\varepsilon(t)$, short dotted line) and ε at last collision point before t (ε(last coll.), dashed line). The eccentricity is calculated using the last interaction points before t. During the time of v_2 growth ($t < 10$ fm/c), ε is large enough to drive v_2 to increase, but this increase is not significant to explain the data at RHIC, while the present model works very well up to SPS energies [30]. The present time-scale of v_2 growth is longer compared to hydrodynamical calculations. For example, momentum anisotropy is shown to grow until $\tau \simeq 2$ fm/c in 2D hydrodynamical

calculation with equation of state (EOS) having the phase transition from QGP to hadron gas [18].

Large spatial eccentricity ε is considered to be a consequence of small p_{T} in the string fragmentation. At the hadronization time, the shift of particle transverse coordinate can be estimated as

$$\Delta r_{\mathrm{T}} \simeq v_{\mathrm{T}} \gamma \tau_{\mathrm{f}} = p_{\mathrm{T}} \tau_{\mathrm{f}} / m. \tag{4}$$

Average $p_{\mathrm{T}} \sim 0.3$–0.4 GeV/c reads $r_{\mathrm{T}} \sim 2$–3 fm for pions, which is not very large compared to the nuclear radius. Thus the elliptic flow can grow slowly also in the hadronic cascade stage. The delay of v_2 growth in hadron-string cascade models would be due to the *dead* time of interaction. Hadrons are formed gradually after $t = \tau_{\mathrm{f}}$, and the γ factor and secondary string-hadron interaction make the delay time longer. Formed hadrons inherit the eccentricity of the original nucleon positions, then v_2 can grow slowly after hadronization.

All the results shown in this paper suggest that in the present hadronic cascade model, the energy is used to increase the number of particles rather than to increase pressure in the early stage compared to the real data. There are several probable reasons for this shortcoming. First one is the change of initial state parton momentum distribution, which comes from the saturation of gluons at low momentum. It is discussed that at very high energies, we can see huge number of gluons at small x, which saturate at some momentum Q_{s} due to gluon fusion, and it may be treated in a classical Yang–Mills field [39]. This saturation reduces the number of gluons at small momenta, and increases the higher momentum gluons. It would be possible to increase the initial pressure in exchange for reducing final hadron multiplicities [40,41]. The next possibility is the partonic re-scatterings just after the initial mini-jet production. Generally, partons produced in mini-jets have large transverse momenta, which may be transferred to longitudinal momenta if they collide with other hadrons. The third candidate is the coherence in the initial mini-jet production. In the present model, we calculate mini-jet production at each NN collision rather than estimating the number of collisions through the thickness of nuclei in the eikonal approximation as in HIJING [37].

4. Summary and discussion

In this work, we have studied the elliptic flow at RHIC by using a jet implemented hadron-string cascade model (JAM). We have compared the calculated results of v_2 with data as a function of pseudo-rapidity, transverse momentum, and centrality. We find that the final hadronic yields are qualitatively described. The elliptic flow v_2 is reasonably well described at low transverse momentum ($p_{\mathrm{T}} < 1$ GeV/c) in mid-central collisions. However, this model is found to undervalue v_2 at high p_{T} or in peripheral collisions. As a result, this model decreases v_2 values as a function of pseudo-rapidity by about 30% and v_2 as a function of transverse momentum for $p_{\mathrm{T}} > 0.5$ GeV/c by about 10–40%, for minimum bias events. The calculated elliptic flows at SPS and RHIC energies are found to be similar, and the reason of this similarity is discussed in terms of spatial eccentricity.

In the analysis of pseudo-rapidity dependence for minimum bias events, the elliptic flow is calculated to be almost constant in the pseudo-rapidity region $|\eta| < 2$ in the present model calculation. Since similar behaviour is found also in the 3D hydrodynamical calculation [19], quick decrease of v_2 at larger η may be due to non-equilibrium dynamics.

Hadronic description seems to fail at high transverse momentum ($p_{\mathrm{T}} > 0.5$ GeV/c for minimum bias events, and $p_{\mathrm{T}} > 1$ GeV/c for mid-central collisions). Since the spatial eccentricity quickly goes down for high momentum particles, especially in peripheral collisions where the participant size is small, it cannot give strong pressure effects on those particles. Similar feature was observed from the analysis of radial flow in the central collisions [7,42]. Thus the elliptic flow at high momenta seems to be actually sensitive to the thermalization in the early stage, and the above observations indicate that it is necessary to include additional processes which are effective in early thermalization than hadron-string cascade processes.

We have also shown the comparison of the calculated elliptic flow results at SPS and RHIC energies. At SPS energy, the elliptic flow as a function of p_{T} is calculated to be very similar to that at RHIC in the present model. Up to SPS energies, we already know that hadron-string description works quite nicely for directed and elliptic flows [31,30]. While the cascade model generally overestimate the elliptic flows, repulsive mean field effects suppress the elliptic flow values and we can explain the data quantitatively at AGS energies [31]. At SPS energies of 40–158 A GeV, mean-field effects are still important to reduce the elliptic flows [30].

In summary, we find that a hadron-string cascade model generally underestimates the elliptic flow at RHIC energy. It may be stated that the natural explanation of this undervalues is to assume that partons produced in mini-jets interact frequently in the early stage at mid-rapidities and thermalized QGP is formed through these re-scatterings, which is not included in the present model.

Acknowledgements

Authors would like to thank Y Nara for fruitful discussions. One of the authors (MI) would like to thank PHENIX group at Univ. of Tsukuba for fruitful discussions. This work was supported in part by the Grant-in-Aid for Scientific Research (No. 1554024) from the Ministry of Education, Science and Culture, Japan.

References

[1] L Liu, Y Deng and Y Hu, *Phys. Lett.* **B388**, 10 (1996); *Proc. Conf. Quark Matter '02* (Nantes, France); *Nucl. Phys.* **A715**, 1c (2003) ; *Proc. Conf. Quark Matter '04* (Oakland, USA); *J. Phys.* **G30**, S1 (2004)
[2] J A Zingman *et al*, *Phys. Rev.* **C38**, 760 (1988)
[3] J Y Ollitrault, *Phys. Rev.* **D46**, 229 (1992)
[4] STAR Collaboration: K H Ackermann *et al*, *Phys. Rev. Lett.* **86**, 402 (2001)
[5] STAR Collaboration: C Adler *et al*, *Phys. Rev. Lett.* **87**, 182301 (2001)
[6] STAR Collaboration: C Adler *et al*, *Phys. Rev. Lett.* **87**, 112303 (2001)
[7] N Xu and M Kaneta, *Nucl. Phys.* **A698**, 306 (2002)

[8] STAR Collaboration: C Adler *et al*, *Phys. Rev.* **C66**, 034904 (2002)
[9] PHENIX Collaboration: K Adcox *et al*, *Phys. Rev. Lett.* **86**, 3500 (2001)
[10] PHENIX Collaboration: K Adcox *et al*, *Phys. Rev.* **C69**, 024904 (2004)
[11] PHOBOS Collaboration: B B Back *et al*, *Phys. Rev. Lett.* **87**, 102303 (2001)
[12] PHOBOS Collaboration: B B Back *et al*, *Phys. Rev. Lett.* **89**, 222301 (2002)
[13] BRAHMS Collaboration: L G Bearden *et al*, *Phys. Lett.* **B523**, 227 (2001)
[14] P F Kolb *et al*, *Phys. Lett.* **B459**, 667 (1999); **B500**, 232 (2001)
[15] P F Kolb *et al*, *Nucl. Phys.* **A696**, 175 (2001)
P Huovinen *et al*, *Nucl. Phys.* **A698**, 475 (2002)
[16] P Huovinen *et al*, *Nucl. Phys.* **B503**, 58 (2001)
[17] J Adams *et al*, *Phys. Rev.* **C72**, 14904 (2005)
[18] P F Kolb, nucl-th/0304036
[19] T Hirano, *Phys. Rev.* **C65**, 011901 (2002)
[20] FOPI collaboration: A Andronic *et al*, *Nucl. Phys.* **A661**, 333 (1999)
[21] E895 Collaboration: P Chung *et al*, *Phys. Rev.* **C66**, 021901 (2002)
[22] NA49 Collaboration: H Appelshauser *et al*, *Phys. Rev. Lett.* **80**, 4136 (1998)
NA49 Collaboration: C Alt *et al*, *Phys. Rev.* **C68**, 034903 (2003)
[23] H Sorge, *Phys. Rev.* **C52**, 3291 (1995)
[24] Y Nara, N Otuka, A Ohnishi, K Niita and S Chiba, *Phys. Rev.* **C61**, 024901 (2000)
[25] E L Bratkovskaya, W Cassing and H Stocker, *Phys. Rev.* **C67**, 054905 (2003)
[26] E E Zabrodin, C Fuchs, L V Bravina and A Faessler, *Phys. Lett.* **B508**, 184 (2001)
[27] Z Lin and C M Ko, *Phys. Rev.* **C65**, 034904 (2002)
[28] A M Poskanzer and S A Voloshin, *Phys. Rev.* **C58**, 1671 (1998)
[29] A M Poskanzer, nucl-ex/0110013 (2001)
N Borghini, P M Dinh and J Y Ollitrault, *Phys. Rev.* **C64**, 054901 (2001)
[30] M Isse, A Ohnishi, N Otuka, P K Sahu and Y Nara, *Phys. Rev.* **C72**, 064908; nucl-th/0502058 (2005)
[31] P K Sahu and W Cassing, *Nucl. Phys.* **A712**, 357 (2002)
P K Sahu, W Cassing, U Mosel and A Ohnishi, *Nucl. Phys.* **A672**, 376 (2000)
P K Sahu, A Hombach, W Cassing, M Effenberger and U Mosel, *Nucl. Phys.* **A640**, 493 (1998)
[32] T Sjöstrand, *Comp. Phys. Comm.* **82**, 74 (1994)
[33] J Sollfrank *et al*, *Phys. Rev.* **C59**, 1637 (1999)
[34] S A Bass *et al*, *Prog. Part. Nucl. Phys.* **41**, 225 (1998)
[35] Y Pang, T J Schlagel and S H Kahana, *Phys. Rev. Lett.* **68**, 2743 (1992)
[36] S Daté, K Kumagai, O Miyamura, H Sumiyoshi and X Z Zhang, *J. Phys. Soc. Jpn.* **68**, 2743 (1995)
[37] X N Wang and M Gyulassy, *Comp. Phys. Comm.* **83**, 307 (1994)
X N Wang, *Phys. Rep.* **280**, 287 (1997)
[38] S C Phatak and P K Sahu, *Phys. Rev.* **C69**, 024901 (2004)
[39] L D McLerran and R Venugopalan, *Phys. Rev.* **D49**, 2233 (1994); *Phys. Rev.* **D49**, 3352 (1994); *Phys. Rev.* **D50**, 2225 (1994)
[40] D Kharzeev and E Levin, *Phys. Lett.* **B523**, 79 (2001)
[41] A Krasnitz, Y Nara and R Venugopalan, *Phys. Rev. Lett.* **87**, 192302 (2001)
[42] N Otuka, P K Sahu, M Isse, Y Nara and A Ohnishi, nucl-th/0102051 (2001)